Communication

New Design of Beam-Formed Leaky-Wave Antenna Based on Substrate Integrated Waveguide in a Confined Space

Yunjie Geng, Junhong Wang, Yujian Li, Zheng Li, Meie Chen, and Zhan Zhang

***Abstract*— A novel design of leaky-wave antenna (LWA) with beam-formed radiation pattern based on substrate integrated waveguide (SIW) is proposed in this communication. The design is based on the idea of superposing radiations from the $n = -1$ space harmonic of different periodic structures in a weighting way. The effect of structural parameters on the radiation performance is first studied using Fourier transform. Then, different periodic structures are mapped into a final composite structure to realize the desired radiation pattern, which is set to be a secant distribution according to the features of long straight confined space considered in this communication. Moreover, a novel double-layer SIW feeding network is proposed and used to construct an LWA array to improve the efficiency and gain. Simulated results are compared with experimental results to validate the proposed idea and design.**

***Index Terms*— Beam-formed pattern, confined space, Fourier transform, leaky-wave antenna (LWA), periodic structure, substrate integrated waveguide (SIW).**

I. Introduction

Nowadays, mobile communication has been extended to various complex environments to meet the requirements of people for full coverage of communication, especially for communication in a confined space, such as tunnels, mines, and other long straight confined spaces [1]. The quality and reliability of wireless communication in a confined space depend mainly on the uniformity of radio wave coverage, which is further dominated by the properties of the antenna installed in the confined space [2]. At present, only a few kinds of antennas, such as the Yagi antenna, helical antenna, and patch antenna whose radiation patterns usually have wide beamwidths, are used in the confined space [3]. When these kinds of antennas are mounted in the confined space with hard boundaries, a large amount of energy will be directly radiated into the nearby hard boundaries, which results in strong reflections and large radio wave fluctuation. All these problems will reduce the system efficiency [4]. To improve the efficiency of the communication system in a confined space, it is necessary to study the mechanism of the radio wave coverage in the confined space and to know how the antenna affects the field distribution, moreover, to design a specifically beam-formed antenna according to the features of a long straight confined space.

Leaky-wave antennas (LWAs), which work on traveling wave, have attracted extensive attention recently because of their well-known features, such as high directivity, simple feeding network, and capability of frequency scanning [5]. The desired radiation pattern as we know can be synthesized by precisely controlling the aperture distribution of the LWA. Some methods have been adopted in the design of LWAs for sidelobe level (SLL) reduction and radiation null generation. In [6], a method of pattern synthesis was proposed based on the iterative Fourier technique for generating nulls in the radiation pattern, in which the propagation constant and the leakage factor of the leaky-wave structure were controlled by aperture tapering technique. In [7], by meandering the long slot in the top wall of the waveguide or meandering the arrays of via holes while keeping the slot in straight, Taylor aperture field distribution was realized, and LWAs with low SLL were obtained. In [8], a new radiation pattern control approach was proposed based on the theory of effective radiation sections, and LWAs with low SLL and wide nulls were realized. However, these available works are only efficient in the reduction of the SLL or generation of the nulls of the LWAs. To our knowledge, for the design of LWAs with specific desired beam-formed patterns, only a few studies based on slot array structure are found. In [9], a double-layer beam-shaped traveling-wave slot array with a nonuniformly slotted configuration was proposed, but the synthesis method and optimization process were abstract and complicated. In addition, traditional substrate integrated waveguide (SIW) LWAs are usually designed based on fundamental wave radiation [10]–[13], but the beam direction of these antennas cannot be changed significantly by the slot period.

In [14], the superposition of radiations of the $n = -1$ space harmonic of different periodic structures was preliminarily studied, and a transversely nonuniformly slotted LWA array with the broad-beam pattern was designed [15]. In this communication, a novel beam-formed LWA based on the SIW [16]–[18] is proposed and designed, using the concept of superposing radiations of the $n = -1$ space harmonic of different periodic structures in a weighting way. Meanwhile, a double-layer SIW feeding network for improving the efficiency is also proposed to feed the LWA array. The method of pattern synthesis in this communication can be seen as a model-driven synthesizing method, while the conventional one can be seen as the data-driven synthesizing method. The theory and method of this communication are introduced in Section II, and detailed design procedures of the beam-formed antenna are given in Section III. The beam-formed patterns of the LWA and the double-layer feeding structure are given in Section IV, in which the experimental results are also given for verification. Finally, the conclusion is drawn in Section V.

II. Theory and Method

As is well known, for a leaky rectangular waveguide with periodic slots cut in the top wall, a lot of spatial harmonics will be generated, among which only those with propagation constant smaller than that of free space can leak away from the structures. Different beam directions of the $n = -1$ space harmonic θ_{-1} can be realized by changing the period of slots P, as shown in Fig. 1(a)–(c). Using this principle, we first design a series of leaky-wave structures with

Manuscript received June 8, 2017; revised April 3, 2018; accepted April 17, 2018. Date of publication August 24, 2018; date of current version October 29, 2018. This work was supported by the National Natural Science Foundation of China under Grant 61331002. *(Corresponding author: Junhong Wang.)*

The authors are with the Key Laboratory of All Optical Network and Advanced Telecommunication Network of Ministry of Education, Beijing Jiaotong University, Beijing 100044, China, and also with the Institute of Lightwave Technology, Beijing Jiaotong University, Beijing 100044, China (e-mail: 15111009@bjtu.edu.cn; wangjunh@bjtu.edu.cn).

Color versions of one or more of the figures in this communication are available online at http://ieeexplore.ieee.org.

Digital Object Identifier 10.1109/TAP.2018.2867018

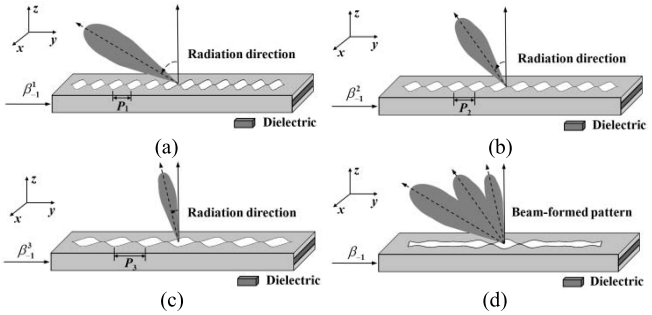

Fig. 1. Basic principle of the proposed beam-formed approach. (a) LWA with periodic slot P_1. (b) LWA with periodic slot P_2. (c) LWA with periodic slot P_3. (d) Beam-formed LWA with a composite slot.

different slot periods, the $n = -1$ space harmonic of these structures is radiating in different directions, then we superpose these radiations in a weighting way (the weighting factors are determined from the desired radiation pattern), and we get a radiation pattern that is similar to the given radiation pattern. For realistic applications, we must map these leaky structures with different slot periods into one structure, as schematically shown in Fig. 1(d). Therefore, the key problem is to superpose different periodic slot structures into one composite slot structure (also in a weighting way). The weighting factors used in the radiation field superposition and structure superposition are the two different sets of weighting functions, and the relationship between them should be found first. The key is to find the relationship between the radiation field and structure parameters, which is obtained by full-wave simulation and Fourier transform in this communication. When the weighting factors for structure superposition are found, the final antenna structure is obtained.

III. Design Procedures

The design procedure of the proposed beam-formed LWA can be composed of four parts as follows.

A. Determination of Beam Angles of the $n = -1$ Space Harmonic From the Given Radiation Pattern

Using the proposed beam-formed method, we choose three different periodic structures, which generate $n = -1$ space harmonic radiating in different directions, to be superposed as shown in Fig. 1. According to the application requirements of this communication, radiation generated by antennas is expected to uniformly cover the long straight confined space. Therefore, the given radiation pattern is set to be a secant distribution radiation pattern: $E = 1/\cos\theta = \sec\theta$. θ is the wide angle of the wave-covered region. E is the normalized radiation electric field in the corresponding direction (the radiation field in the normal direction is selected as the reference value). The radiations from the three structures are superposed to form the given pattern.

However, in practice, the superposition of three beams can be carried out with different beamwidths as shown in Fig. 2, i.e., half-power beamwidth (HPBW) [Fig. 2(a)], first-null beamwidth (FNBW) [Fig. 2(b)], or an arbitrary beamwidth $\Delta\theta_n$ (n = 1, 2, 3) [Fig. 2(c)]. Because of significant beam overlapping, the case of Fig. 2(a) requires the control of the phase in each beam, which is challenging to obtain. Furthermore, the case of Fig. 2(b) would result in multiple radiation nulls. It is found empirically that a beamwidth of $\Delta\theta_n$ is defined as

$$\Delta\theta_n \approx \frac{1.15}{(Ls/\lambda_0)\cos\theta_n} \tag{1}$$

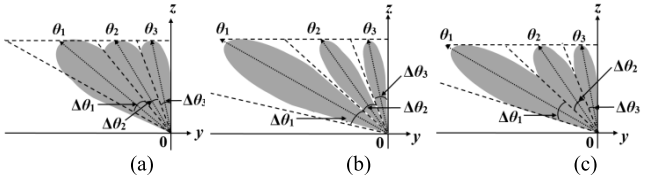

Fig. 2. Three cases of beam superposition, $\Delta\theta_n$ (n = 1, 2, 3) are defined, respectively, by (a) HPBW, (b) FNBW, and (c) certain beamwidth in between HPBW and FNBW.

TABLE I
Theoretical Results of Beam Angles and Beam Widths When $Le = 3.5$

n	1	2	3
$\Delta\theta_n$	36.7°	21.7°	19.1°
θ_n	-59.15°	-29.95°	-9.55°

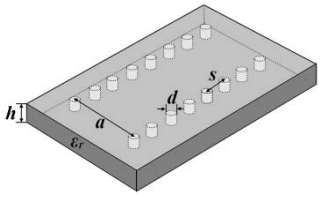

Fig. 3. Configuration of the basic structure of SIW.

whose value is between HPBW and FNBW can yield a pattern close to the secant distribution. And the relationship between the beam angle θ_n and the beamwidth $\Delta\theta_n$ can be approximately expressed as

$$\begin{cases} \theta_3 = \Delta\theta_3/2 \\ \theta_2 = \Delta\theta_2/2 + \Delta\theta_3 \\ \theta_1 = \Delta\theta_1/2 + \Delta\theta_2 + \Delta\theta_3. \end{cases} \tag{2}$$

Therefore, when the wavelength λ_0 and slot length Ls are given, the beam angles θ_n and beam widths $\Delta\theta_n$ of these three beams in Fig. 2(c) can be calculated by (1) and (2). In this design, we choose the electric length $Le = Ls/\lambda_0 = 3.5$ to get a wide coverage of radiation field, then the theoretical results of the three beam angles and the corresponding beam widths are obtained, as listed in Table I.

B. Design of SIW LWAs for Different Beam Angles of the $n = -1$ Space harmonic

The basic structure of SIW in our design is shown in Fig. 3. The dielectric is set to Rogers RO 3003 with a thickness of $h = 1.524$ mm, the permittivity of $\varepsilon_r = 3.0$, and the loss tangent of $\tan\delta = 0.0013$. The diameter of metalized vias is $d = 0.9$ mm and the space between the adjacent vias is $s = 1.6$ mm. The width of this SIW is $a = 9.6$ mm, which makes sure that the SIW works in TE_{10} mode at the operating frequency of $f = 17.5$ GHz.

There are many types of slots used to construct the periodic structure; the simple and commonly used one is the transverse slot [10], [11]. In this communication, we propose a new kind of SIW LWA with periodic slot whose shape is designed according to the cosine function, as shown in Fig. 4. There are two reasons for choosing this cosine-shaped slot rather than the transverse slot. First, the cosine-shaped slot is a periodic structure just like the periodic transverse slot; so, when the period of function changes (corresponding to the change of slot period), the beam angle of the $n = -1$ space harmonic will change too. Second, when compared

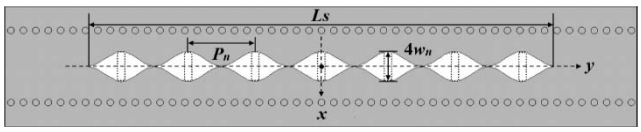

Fig. 4. Structure of the SIW LWA with the cosine-shaped slot.

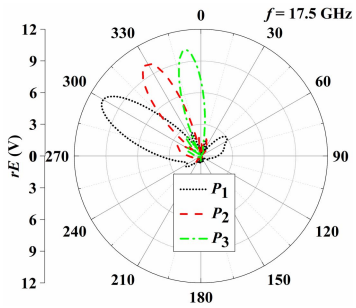

Fig. 5. Simulated radiation patterns ($\varphi = 90°$) of the SIW LWAs with different periodic cosine-shaped slots as shown in Fig. 4.

TABLE II
SIMULATED RESULTS OF THE SIW LWAS WITH DIFFERENT PERIODS OF COSINE-SHAPED SLOT

n	1	2	3
P_n (mm)	7.8	9.3	11.2
θ_n	-60°	-30°	-10°

with the transverse slot, the cosine-shaped slot has a relatively continuous structure, which ensures the gradual change of characteristic impedance of the leaky waveguide, and the strong reflections at resonant frequencies can be avoided. Moreover, for the method proposed in this design, the mode in the waveguide is required to be almost the same with the phase constant almost unchanged; therefore, it may not be applied for the transversely slotted structures, whose phase constant changes significantly with the period of slots.

In this communication, the expression of the cosine function is

$$x = w_n \times \cos\left(\frac{2\pi}{P_n} \times y\right) + w_n, -Ls/2 \le y \le Ls/2, \quad n = 1, 2, 3 \tag{3}$$

where w_n is the weighting factor of each cosine function. Moreover, $4w_n$ is defined as the maximum width of the slot, as indicated in Fig. 4, which affects the radiation strength of the antenna directly. P_n is the period of the cosine function, which is also the period of the slot. Ls is the total length of the cosine-shaped slot and is set to 60 mm in this communication.

The slot period P_n should meet the condition of monoradiation of the $n = -1$ space harmonic, which can be calculated corresponding to the three beam angles θ_n in Table I. The radiation patterns (calculated at far-field region and in plane of $\varphi = 90°$) of these three SIW LWAs with the designed periods of cosine-shaped slots are obtained, respectively, as shown in Fig. 5. The radiation strengths in Fig. 5 are not weighted yet, which means that all w_n are set to 1 in the simulation. It can be found that the radiation patterns of these three antennas with different periodic slots are basically consistent with our design presented in Section III-A. The detailed information of these three simulated beams is summarized in Table II.

C. Relationship Between the Radiation Field and the Structure Parameter

The radiation pattern can be found by taking the Fourier transform of the aperture field distribution as we know from [5], and the aperture field E_n is further affected by the slot width w_n. Therefore, to find the relationship between w_n and E_n, the three cosine-shaped slotted LWAs with different slot widths are simulated. Then, by taking the Fourier transform of the field distribution along the slot aperture, we can find the Fourier coefficient of the $n = -1$ space harmonic A^n_{-1}, which reflects the radiation strength of the electric field E_n directly. The variation of slot width also causes the change of phase constant β_{-1}; however, the change of β_{-1} due to the variation of w_n is small and can be neglected when compared with that due to the change of P_n [12].

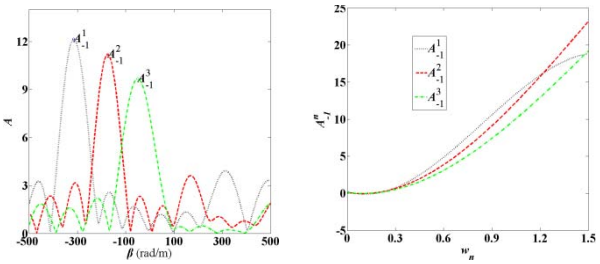

(a) (b)

Fig. 6. Variations of Fourier coefficients of the $n = -1$ space harmonic A^n_{-1} as functions of (a) propagation constant β when $w_n = 1$ and (b) weighting factors w_n, for the three LWAs with different slot periods P_n, $n = 1, 2, 3$.

Fig. 6(a) gives the relationship between Fourier coefficient and propagation constant for different slot periods when $w_n = 1$, where A^1_{-1}, A^2_{-1}, and A^3_{-1} are the Fourier coefficients of the $n = -1$ space harmonic for $P_1 = 7.8$ mm, $P_2 = 9.3$ mm, and $P_3 = 11.2$ mm, respectively. By changing w_n, we can get a series of photographs like Fig. 6(a), from which we can obtain the relationships between the Fourier coefficients of the $n = -1$ space harmonic A^n_{-1} and the weighting factors w_n, $n = 1, 2, 3$. The results are shown in Fig. 6(b), which also represent the relationship between the structure parameters of LWAs and the radiation fields.

D. Selection of the Weighting Factors and Structure of the Composite Slot Antenna

As discussed in Section III-A, the relationships between the normalized radiation electric fields E_n and the beam directions of the $n = -1$ space harmonic θ_n of three LWAs should be designed to meet the secant function as in the following relationships:

$$E_1 : E_2 : E_3 = \sec\theta_1 : \sec\theta_2 : \sec\theta_3 \tag{4}$$

Because of the proportional relationship between the radiation electric fields E_n and Fourier coefficients A^n_{-1}, (4) can be rewritten as

$$A^1_{-1} : A^2_{-1} : A^3_{-1} = \sec\theta_1 : \sec\theta_2 : \sec\theta_3. \tag{5}$$

Then, using (5) and Fig. 6(b), the slot widths of the three periodic structures can be easily obtained according to the given radiation pattern. In other words, the weighting factor w_n for each cosine function in (3) can be found.

Because (5) only gives the relative ratios, we have many choices for the specific values of Fourier coefficientsA^n_{-1} and the weighting factors w_n. In this design, we select them based on the simulated results of the radiation pattern and the input impedance. Once the weighting factors w_n are found, the final composite cosine-shaped slot can be expressed as

$$x = \frac{1}{3}\sum_{n=1}^{3}\left[w_n \times \cos\left(\frac{2\pi}{P_n} \times y\right) + w_n\right] \quad -Ls/2 \le y \le Ls/2, \quad n = 1, 2, 3 \tag{6}$$

TABLE III
PARAMETERS OF THE COMPOSITE COSINE-SHAPED SLOT

n	1	2	3
P_n (mm)	7.8	9.3	11.2
w_n	1.2870	0.9375	0.9745

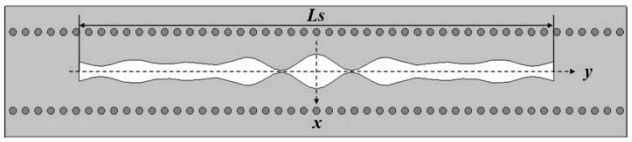

Fig. 7. Structure of the beam-formed SIW LWA with the composite cosine-shaped slot.

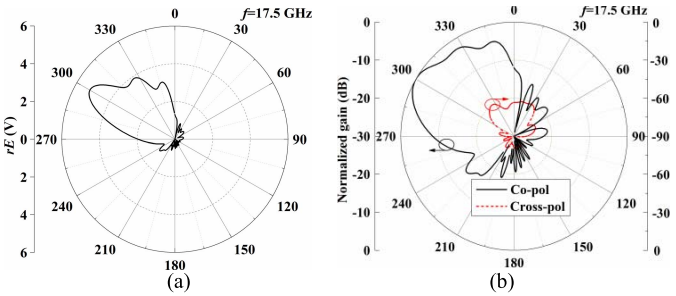

Fig. 8. Simulated radiation patterns ($\varphi = 90°$) of the beam-formed SIW LWA. (a) Field radiation pattern. (b) Normalized gain pattern.

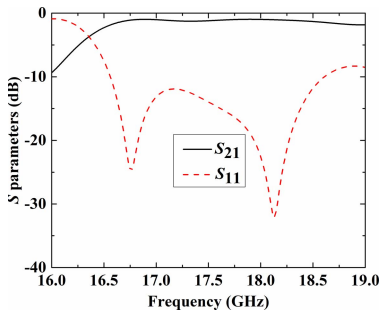

Fig. 9. Simulated S-parameters of the beam-formed SIW LWA.

where P_n are the periods of the cosine-shaped slots and w_n are the final weighting factors, which are given in Table III. Considering that the width of the superposed composite slot should not be larger than that of the waveguide, a divisor equal to the number of superposed beams is used in (6). Fig. 7 shows the final structure of the proposed beam-formed SIW LWA with the composite cosine-shaped slot.

IV. RESULTS AND DISCUSSION

A. Simulated Results of the Proposed Beam-Formed SIW LWA

The simulated radiation patterns ($\varphi = 90°$) of the designed antenna in Fig. 7 are plotted in Fig. 8(a) and (b) which shows the field radiation pattern and the normalized gain pattern, respectively. It can be seen from Fig. 8(a) that there are three beams approximately pointing to $-60°$, $-30°$, and $-10°$, respectively, and the whole pattern is formed by them. In addition, although the distribution of the radiation field does not match the desired secant distribution completely, it is very close to that one.

The simulated S parameters of the beam-formed antenna are depicted in Fig. 9, from which we observe that S_{11} is less than -10 dB within a wideband from 16.5 to 18.5 GHz. However, S_{21} within the passband is only about -1 dB, which indicates that most of the transmitted power is absorbed by the matching load; so, the radiation efficiency is quite low. There are two reasons for the low radiation efficiency. First, the length of the slot *Ls* is not long enough to leak most of the power. Second, as we can see from Fig. 7, the composite cosine-shaped slot is a symmetric structure cut in the middle of the top wall. Therefore, the excitation of the aperture field of this structure is not as good as that of the asymmetry structures [19]. Therefore, an approach of efficiency improvement is proposed in Section IV-B.

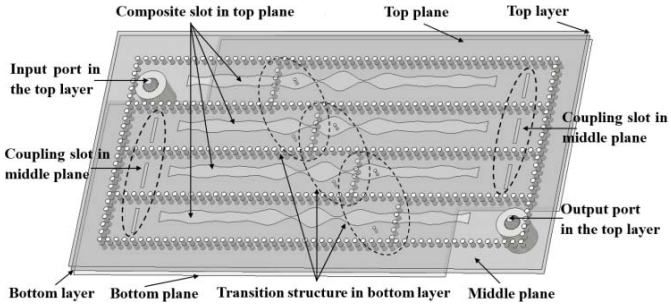

Fig. 10. Configuration of the double-layer SIW LWA array.

B. Efficiency Improvement of the Composite Cosine-Shaped Slot Antenna

Several types of LWAs with series feeding network to improve radiation efficiency have been proposed previously. Nguyen *et al.* [20] gave a high-efficiency LWA array that recycles the power at the output port of the center element back into the input ports of the neighboring elements using additional power divider and cables. Geng *et al.* [11] presented a novel solution to improve the radiation efficiency of LWAs by using the hybrid radiation of fundamental wave and the $n = -1$ spatial harmonic of the leaky waveguide. When compared with these two methods, the double-layer SIW LWA array proposed here is more compact and simple.

Fig. 10 demonstrates the whole geometry of this double-layer SIW LWA array, the composite cosine-shaped slot is cut in the top plane of the top layer, and the feeding network is designed in the bottom layer. The basic SIW structure of this array is the same as that in Fig. 3. The substrate of both layers has the same thickness and dielectric constant, as those of the single SIW LWA. The whole antenna array consists of three parts, that is, four single LWAs with composite cosine-shaped slots at the top layer, six coupling slots in the middle plane between the two layers, and three transition structures in the bottom layer. The working principle of this array is the same as that proposed in [21].

The radiation patterns in H-plane and E-plane of the double-layer SIW LWA array are shown in Fig. 11. And the simulated radiation patterns of the single SIW LWA are also given for comparison. It is observed from Fig. 11(a) that the radiation pattern of the array is basically the same as that of the single beam-formed SIW LWA. However, the ripples caused by the superposition of three beams are not so obvious because of the mutual coupling between four LWAs. Moreover, the field strength of the array is much larger than that of the single LWA, which indicates that the gain, as well as the radiation efficiency, has been improved significantly. Meanwhile, as shown in Fig. 11(b), the beamwidth in E-plane (passing through the maximum radiation direction) of the array is smaller than that of the single LWA.

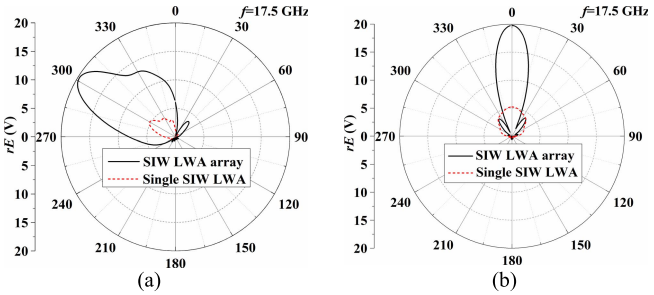

Fig. 11. Simulated radiation patterns of the SIW LWA array and the single SIW LWA. (a) H-plane. (b) E-plane (passing through the maximum radiation direction).

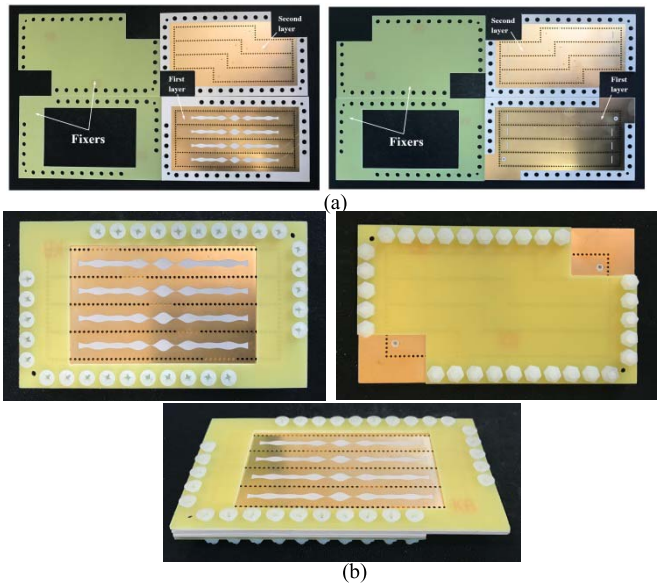

Fig. 12. Fabricated prototype of the double-layer array. (a) Photographs of the front view and back view of the separated parts. (b) Photographs of the front view, back view, and perspective view of the whole assembled structure.

The fabricated prototype of the double-layer SIW array is shown in Fig. 12, where Fig. 12(a) is the photograph of separated parts and Fig. 12(b) is the photograph of the whole assembled structure whose size is 100×60 mm^2. As we can see, the top layer and bottom layer are assembled together by using two fixers and a number of screws, which have little effect on the performance of the array if appropriately designed. Fig. 13 shows the simulated and measured S parameters of this array. Because the manufacturing tolerance in the coaxial probe feeding structure is not easy to control exactly as that we designed, the measured S_{11}, which is around -10 dB in the working frequency, is not as good as the simulated one, and the measured S_{21} is much smaller than the simulated one. In addition, the errors in the processing of assembly and measurement are the other reasons of the discrepancies between the simulated and measured results.

Fig. 14 depicts the simulated and experimental copolarization and cross-polarization radiation patterns ($\varphi = 90°$) of the proposed array at the frequency of 17.5 GHz. It is observed that there are some discrepancies between the simulation and measurement patterns, especially for the sidelobes and backlobes. Because of the manufacturing tolerances in the substrate parameters and some errors in the measurement process, the performances of a realistic antenna would be affected and the measured results would deviate from

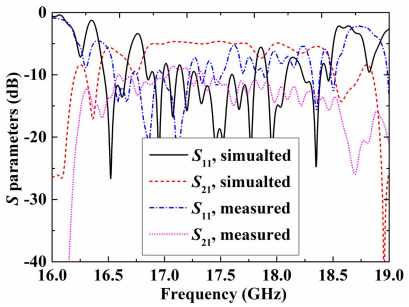

Fig. 13. Simulated and measured S-parameters of the SIW LWA array.

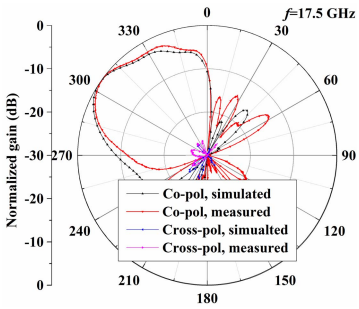

Fig. 14. Simulated and measured normalized copolarization and cross-polarization gain patterns ($\varphi = 90°$) of the SIW LWA array.

TABLE IV
RESULTS OF THE SIW LWA ARRAY AND THE SINGLE SIW LWA AT 17.5 GHz

	SIW LWA array		Single SIW LWA
	Simulated	Measured	Simulated
G (dB)	9.8	7.5	0.01
η_{RAD}	42.17%	n. a.	13.96%
η_{total}	64.59%	81.92%	20.23%

the simulations. However, the main beams of simulated and measured copolarization patterns are in good agreement.

Table IV summarizes the results of this array and the single LWA at the operating frequency. Because of the discrepancies between the simulated and measured return loss as mentioned before, the power reflected the input port in the experiment is larger than that in the simulation. Therefore, the measured gain is lower than that of simulation, as can be seen from Table IV. Although the measured performance of this array is not as good as the simulated results due to the errors of fabrication and measurement, the radiation efficiency and the gain of the proposed array have been significantly improved when compared with those of single LWA, which validates the feeding network proposed in this section. The simulated and measured total power ratios for dissipation and radiation ($\eta_{\text{total}} = 1 - S_{11}^2 - S_{21}^2$) are also given for comparison. As can be seen, the measured total power ratio for dissipation and radiation is higher than the simulation; this is mainly due to the effect of probe feeding connectors used in the experiment, which causes additional loss.

V. CONCLUSION

In this communication, a novel design of beam-formed SIW LWA in a confined space is proposed and validated. The antenna is realized by superposing radiations from the $n = -1$ space harmonic of different periodic structures in a weighting way and can give a field distribution like a secant distribution. To overcome the disadvantage

of low radiation efficiency of the single LWA, a novel double-layer feeding network is proposed and applied to a four-element array. The measured results validate the feasibility of the proposed design. However, when compared with the conventional methods of radiation pattern synthesis, the proposed method still has some limitations, for example, it did not take into account the influence of sidelobe and the mutual coupling when superposing the beams, and it may not be applied for other types of periodic structures. These limitations will be further studied in our future work.

REFERENCES

[1] J. Wang, Y. Huang, and D. Li, "Research on the field coverage generated by antennas in confined space," in *Proc. 3rd Asia–Pacific Conf. Antennas Propag.*, Harbin, China, Jul. 2014, pp. 775–778.

[2] R. He, Z. Zhong, B. Ai, and J. Ding, "An empirical path loss model and fading analysis for high-speed railway viaduct scenarios," *IEEE Antennas Wireless Propag. Lett.*, vol. 10, pp. 808–812, 2011.

[3] C. Briso-Rodriguez, J. M. Cruz, and J. I. Alonso, "Measurements and modeling of distributed antenna systems in railway tunnels," *IEEE Trans. Veh. Technol.*, vol. 56, no. 5, pp. 2870–2879, Sep. 2007.

[4] F. Zhang, "Analysis of antenna radiation characteristics in mine tunnels," in *Proc. 9th Int. Symp. Antennas Propag. EM Theory*, Guangzhou, China, Nov./Dec. 2010, pp. 327–330.

[5] A. Oliner and D. R. Jackson, "Leaky-wave antennas," in *Antenna Engineering Handbook*, J. L. Volakis, Ed. New York, NY, USA: McGraw-Hill, 2007.

[6] J. L. Gómez-Tornero, A. J. Martínez-Ros, and R. Verdú-Monedero, "FFT synthesis of radiation patterns with wide nulls using tapered leaky-wave antennas," *IEEE Antennas Wireless Propag. Lett.*, vol. 9, pp. 518–521, May 2010.

[7] Y. J. Cheng, W. Hong, K. Wu, and Y. Fan, "Millimeter-wave substrate integrated waveguide long slot leaky-wave antennas and two-dimensional multibeam applications," *IEEE Trans. Antennas Propag.*, vol. 59, no. 1, pp. 40–47, Jan. 2011.

[8] Z. Li, J. Wang, M. Chen, and Z. Zhang, "New approach of radiation pattern control for leaky-wave antennas based on the effective radiation sections," *IEEE Trans. Antennas Propag.*, vol. 63, no. 7, pp. 2867–2878, Jul. 2015.

[9] L. Qiu, K. Xiao, S. L. Chai, H. Y. Qi, and J. J. Mao, "A double-layer shaped-beam traveling-wave slot array based on SIW," *IEEE Trans. Antennas Propag.*, vol. 64, no. 11, pp. 4639–4647, Nov. 2016.

[10] J. Liu, D. R. Jackson, and Y. Long, "Substrate integrated waveguide (SIW) leaky-wave antenna with transverse slots," *IEEE Trans. Antennas Propag.*, vol. 60, no. 1, pp. 20–29, Jan. 2012.

[11] Y. Geng, J. Wang, Y. Li, Z. Li, M. Chen, and Z. Zhang, "Leaky-wave antenna array with a power-recycling feeding network for radiation efficiency improvement," *IEEE Trans. Antennas Propag.*, vol. 65, no. 5, pp. 2689–2694, May 2017.

[12] X. Huo, J. Wang, D. Li, Z. Zhang, M. Chen, and Z. Li, "Research on the propagation constant of the periodically slotted rectangular waveguide by equivalent circuit method," *Microw. Opt. Technol. Lett.*, vol. 58, no. 2, pp. 426–429, 2016.

[13] Y. Mohtashami and J. Rashed-Mohassel, "A butterfly substrate integrated waveguide leaky-wave antenna," *IEEE Trans. Antennas Propag.*, vol. 62, no. 6, pp. 3384–3388, Jun. 2014.

[14] J. Wang, Y. Geng, C. Zhang, and X. Huo, "Radiation characteristic of the periodic leaky wave structure and its application to leaky wave antenna design," in *Proc. Asia–Pacific Microw. Conf. (APMC)*, Nanjing, China, Dec. 2015, p. 1.

[15] Y. Geng and J. Wang, "Non-uniform slotted leaky wave antenna array for broad-beam radiation based on substrate integrated waveguide," in *Proc. 11th Int. Symp. Antennas, Propag. EM Theory (ISAPE)*, Guilin, China, Oct. 2016, pp. 159–162.

[16] D. Deslandes and K. Wu, "Design consideration and performance analysis of substrate integrated waveguide components," in *Proc. 32nd Eur. Microw. Conf.*, Milan, Italy, Sep. 2002, pp. 1–4.

[17] Y. Cassivi, L. Perregrini, P. Arcioni, M. Bressan, K. Wu, and G. Conciauro, "Dispersion characteristics of substrate integrated rectangular waveguide," *IEEE Microw. Wireless Compon. Lett.*, vol. 12, no. 9, pp. 333–335, Sep. 2002.

[18] F. Xu and K. Wu, "Guided-wave and leakage characteristics of substrate integrated waveguide," *IEEE Trans. Microw. Theory Techn.*, vol. 53, no. 1, pp. 66–73, Jan. 2005.

[19] C. Caloz and S. Otto, "The symmetry secrets of periodic leaky-wave antennas," in *Proc. Int. Conf. Electromagn. Adv. Appl. (ICEAA)*, Palm Beach, The Netherlands, Aug. 2014, pp. 543–545.

[20] H. V. Nguyen, S. Abielmona, and C. Caloz, "Highly efficient leaky-wave antenna array using a power-recycling series feeding network," *IEEE Antennas Wireless Propag. Lett.*, vol. 8, pp. 441–444, 2009.

[21] Y. Geng and J. Wang, "A novel double-layer leaky-wave antenna array for radiation efficiency improvement based on substrate integrated waveguide," in *Proc. IEEE Int. Symp. Antennas Propag. USNC/URSI Nat. Radio Sci. Meeting*, San Diego, CA, USA, Jul. 2017, pp. 837–838.